Metallurgical and Materials Engineering *Research paper*
https://doi.org/10.56801/MME861

INVESTIGATION OF MICROSTRUCTURE, AND MECHANICAL PROPERTIES OF DISSIMILAR HIGH AND ULTRA-HIGH STEEL WELDED JOINTS: APPLICATION FOR EXTREME CLIMATE CONDITIONS

Francois Njock Bayock [1,], Paul William Huisken Mejouyo[1], Mbelle Samuel Bisong[1], Paul Kah[2]*

[1]Department of Mechanical Engineering, ENSET Douala, University of Douala, P.O. Box: 1872, Douala, Cameroon
[2]Department of Engineering Science, University West, Gustava Melius gata 2 S-461 32 Trollhättan, Sweden

Received 06.07.2022
Accepted 10.12.2022

Abstract

The paper focuses on the technical challenges of producing high-quality welds in modern extreme climate conditions structures, as welds are typically the weakest part of welded structures. Welding is particularly difficult with high-strength and ultra-high-strength steels (HSS-UHSS), which are used in structures to reduce weight. The microstructural compositions and mechanical properties of dissimilar high-strength and ultra-high-strength steels were investigated in this study, which was performed with three different heat inputs (0.8, 1.2, and 1.8 kJ/mm). There was a 2.3Cr, 0.4Si, and 2.8Mn increase on the FGHAZ microstructure of the S960QC side, confirming the temperature increase in that zone. Microhardness results show softening (160 HV5) in the E500 side's fine grain heat-affected zone (FGHAZ). Bending test results show that when the maximum force applied was 4000N, the fracture angle was close to 149°, and that the fracture zone was oriented exclusively in the FGHAZ, which had the higher softening zone. Tensile results show the fracture zone, which was oriented in the E500 side's FGHAZ. It was suggested that a heat input of 1.2 kJ/mm be applied to the weld dissimilar joint of TMCP E500-S960QC, which will be beneficial for extreme climate conditions.

Keywords: Bending test tensile test; EDS microscopy; high strength steel; ultra hight strength steel; extreme conditions; dissimilar welded joints.

[*]Corresponding author: Author Francois Njock Bayock, *njockfm1@outlook.com*

Introduction

Climate change is now threatening the global environment. On one hand, it combats global warming; on the other, the rise in raw material prices causes profound reflections in the fields of renewable energies. The most vulnerable regions (arctic-) deserve strong structures that can withstand climate change. It is therefore critical to identify means and methods for resolving the problem at hand. Materials used in industrial products such as automobiles and wind turbines are very specific. The most commonly used materials today have the advantages of being lighter and stronger. Weld qualities that will be applied to these metals must first be studied and characterized. The process of selecting the type of weld will consider the basic materials to be welded (production process and applicability), the geometry of the weld joint, the welding parameters, and the type of filler metal to be used (if welding with filler metal) [1-4].

The use of dissimilar welds is one solution for reducing the weight of welded structures while also solving the structural strength problem [5-7]. This solution will be resistant to a variety of climatic conditions. For loaded applications requiring a specific yield strength, the lightest and cheapest solution is steel with the highest value of _ym/(Cp), where y is the yield strength, m is the coefficient of loading (1 for simple tension), and C is the cost per unit mass. High-strength steels are more expensive than conventional steel, but the cost rises slower than the strength. In most cases, the cost per unit mass of structural steel can be calculated using the following formula [1]:

$$\frac{C(\sigma_y)}{C(355)} = \left\{\frac{\sigma_y}{355}\right\}^{0,5} \qquad 1$$

According to the above-mentioned equations, if m>0, 5, the result of eq. 1 will indicate an increase with increasing steel strength. As a result, lighter solutions that use higher strength steel can be more efficient and economical. In the review, there are various high-strength steels that can withstand various climate changes. Steel nowadays has the unique property of having good weldability depending on how the welding process and different material properties are combined. The yield strength of the underlying material can reach 1300 MPa. The main concern when welding dissimilar steel joints is to reduce softening in the heat-affected zone [8]. Depending on how the steel was manufactured and the welding process, it may be possible to preheat and apply post-weld heat treatment to the welded sample to reduce the softening area in the HAZ. When welding dissimilar steel structures, many factors contributed to softening and brittle zones in the HAZ. The steel production process must be divided into steps with different phase transformations. The effect of the heating process on the phase transformation of the materials can be the microstructural constituent in the HAZ. According to the literature, the first generation of steel has slightly increased elongation with low yield strength and contains less than 2% Mn. Mild steel, some Martensite steel (MS), conventional high strength steels such as carbon-manganese steels, duplex phase steel (DS), and so on... Second generation steels created a new AHSS steel grade, such as TRIP- Bainite Ferrite, TWIP steel, and lightweight steel with induced plasticity (L-IP). The third generation of AHSS is concerned with steels that have strength-ductility combinations [4]. The complexity of the microstructural morphology is the issue with the third generation of AHSS. In terms of microstructure characterization, work has been completed in the fine grain HAZ and on the coarse grain HAZ. Many heat treatments are

used in the steel manufacturing process. Controlled rolling (CR), which is used to analyze grain size evolution and precipitation strengthening, can control the material's microstructural constituents. Another transformation process noted was the control of thermomechanical processes, which controlled the crystalline structure of the metal. The heat process increases the grain size of the metal, while the cooling process decreases the grain size [8].

Requirements and challenges for welds for extreme climate conditions

Extreme climate conditions, such as those found in Sub-Saharan Africa and the Arctic, make welding difficult; there is a link between welding procedures, methods, and various defects (crack propagation, strengthening area...) in the heat-affected zone [2]. In the literature, there is a requirement for the service temperature in the arctic regions, which can be estimated at -60 °C, and for the sub-Saha region, which can be estimated at 50 °C. In most extreme conditions, the temperature that can be favorable for developing good weldability in welded structures should be less than -40°C and 30°C, respectively, for cold and hot temperature conditions. The materials and welding requirements for floating and stationary offshore platforms and other structures differ significantly. One of the most common cold-resistance tests is the Charpy impact energy test, which determines the impact energy required to break the specimen. To evaluate the impact, the standards generally recommended a required value, which can be calculated as 10% of the yield strength value at the design temperature [9]. When determining the Charpy impact test, it is recommended that the pass weld numbers, austenite grain size, and ferrite volume fraction be considered. To investigate the suitability of TMCP and QT high-strength steels for use in extreme conditions, a literature review was conducted. *Chin-Hyung Lee et al.* [10] investigated the suitability of TMCP steel SM570-TMCP in cold environments and concluded that selecting an appropriate welding process is critical for the operation of TMCP steels in such environments. *Jia-Bao Yan et al.* [10] investigated the mechanical properties of QT S690 steel in extreme conditions and discovered that when S960QT is subjected to low heat input temperatures, yield and tensile yield strength increase. *Shin et al.* [11] conducted additional research on the fracture characteristics of TMCP and QT steels in extreme conditions. They demonstrated that in cold regions, TMCP steel is far preferable to S960 QT steel. It is recommended that the materials be preheated before welding with S690QT. Figure 1a depicts the yield stress function of the ductile-brittle transition temperature (DBTT), which can be used to define the fracture stress limit of a welded joint [12-14]. Figure 1b depicts a typical welding parameter window for welding applications. The graph depicts the risk of crack propagation as heat input increases due to toughness, hardness, and strength. Preheating samples has been discovered to be critical in order to avoid the risk of crack propagation.

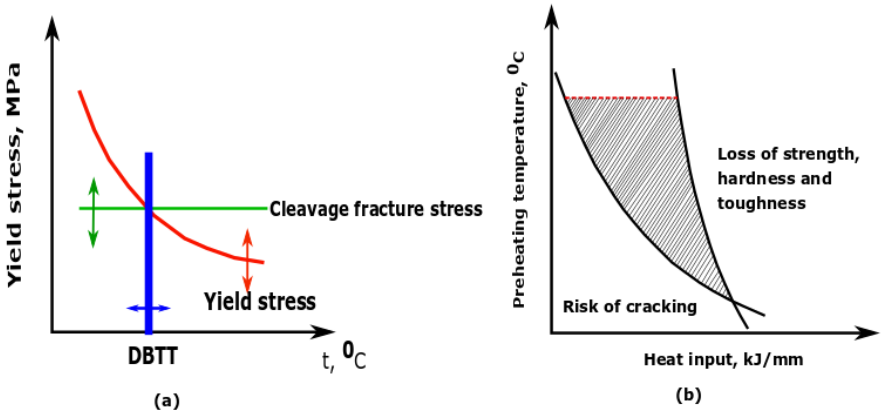

Fig. 1. a - Yoffee diagram; b - Typical welding parameter window for welding applications [15].

Because of their sensitivity to heat input values, the investigated materials (TMCP E500 and S960QC) have weldability issues. Crack propagation will be influenced by increasing the heat input values in the heat-affected zone of the welded joints. The difficulties in welding HSS and UHSS, particularly the relationship between heat input, hardenability, strength behavior, and cold crack propagation [16,17]. In their study, *Raghawendra et al.* [18] investigated the capability of using the electron beam welding (EBW) process while minimizing thermal effect, as well as how the mechanical and microstructural constituents of the HAZ can be affected. The microstructure and mechanical properties of dissimilar welded joints of TMCP E500 and S960QC were investigated in this study using the GMAW process. Microstructure, tensile, and bending tests were carried out to assess microstructural change, hardness, and strength in the HAZ of a dissimilar joint.

Case study

The investigated materials were a dissimilar welded joint of thermo mechanically controlled processes steel E500 and Thermo mechanic Optim 960QC steel grade, which is a rage of lighter structures. To weld samples, GMAW presses were applied. Three heat input values were applied to weld a sample (0.8, 1.2, and 1.8 kJ/mm). Three specimens of a dissimilar joint plate having dimensions of 150 mm x 50 mm. The steel plate had a thickness of 8mm, equipped with a V-groove geometry of joint, and 2 passes. The joint angle performed was 60 ° with a gap of 2 mm. Figure 2 shows one welded joint specimen performed.

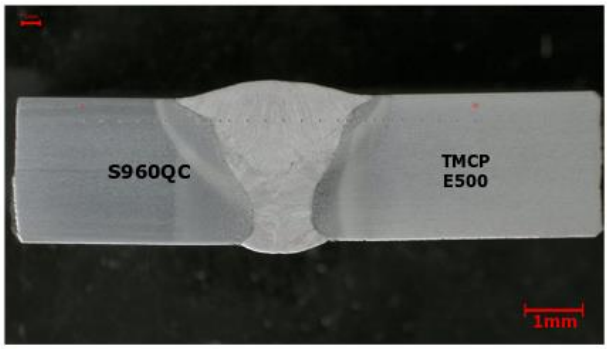

Fig. 2. Performed cross-section of dissimilar TMCP E500 and S960QC.

The influence of thermal diffusion on the microstructural constituent, the formation of alloying elements in the coarse grain HAZ, and the mechanical properties of the different welded joint specimens will be determined from the thermal cycle using different heat input values. A microstructure analysis using an energy-dispersive X-ray spectroscopy test with a data type (Weight%), image resolution of 1024 by 768, image Pixel Size of 0.02 µm, the Map resolution of 256 by 192, Map Pixel Size of 0.07µm, the acc. HV5 microhardness measurements were performed using a Wilson Wopert 452SVD Vickers hardness tester and a voltage of 20.0 kV and a magnification of 7499 in accordance with ISO 6507-1:2018. Bending tests were carried out with the help of standard VDA 238-100 bending test equipment. The tensile test was carried out using ZWICK/ROZ Z 330 RED equipment (Zwick Rowell, Ulm, Germany) (Figure 3). The maximum load capacity used was 100 kN, in accordance with the EN ISO 6892-1:2016 standard [19]. Tables 1 and 2 show the chemical composition, mechanical properties of the based materials (TMCP E500 and Optim 960QC) and filler wire, as well as welding parameters.

The material behavior was tested using a frictionless bending test setup in accordance with the SFS-EN ISO 7438:2016 standard [20]. The standard VDA 238-100 bending test equipment is shown in Fig. 4 below. In the experimental procedure, tree points were exanimated to investigate a surface weld test (FBB) and a branching knife root bending test (RBB). The bending test operation, the sample, the console, and the computer for data analysis and saving can all be seen in the figure.

The carbon equivalent values (CEV) of the investigated steels (E500, S960QC, and filler wire) were calculated according to EN 1011-2:2001 annex C, Method A [18, 21]:

$$CEV = C + \frac{Mn}{6} + \frac{Cr+Mo+V}{5} + \frac{Ni+Cu}{15} \qquad 2$$

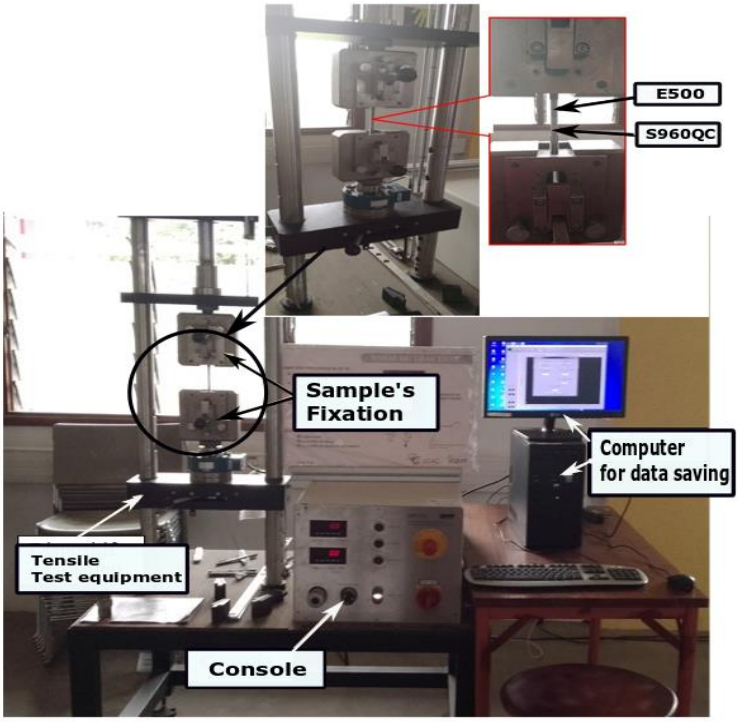

Fig. 3. Tensile test equipment using ZWICK/ROZ Z 330 RED equipment (Zwick Rowell, Ulm, Germany).

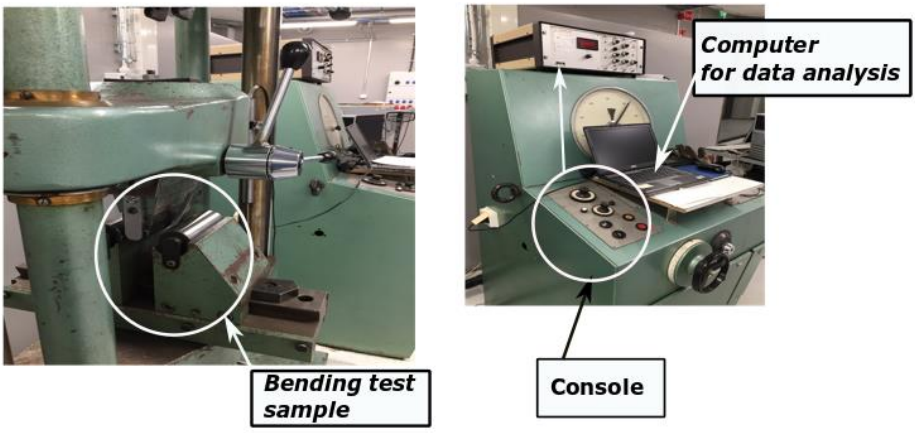

Fig. 4. Standard VDA 238-100 bending test equipment.

From Table 1 and Table 2, the required and the measurement of chemical composition and mechanical properties of both materials were set up according to EN 10204 3.1material certificate (provided by the steel producer).

Table 1. TMCP E500 (European steel manufacturing by Rautaruukki Oy) and S960QC (EN 10051) steel microstructure composition and mechanical properties, and filler material NiCrMo700.

Chemical composition, wt %.																
	C	Si	Mn	Al	B	Nb	Ti	V	Cu	Cr	Ni	Mo	N	P	S	CEV
TMCP E500	0.08	0.25	1.50	0.053	-	0.035	0.018	0.008	0.15	0.05	0.90	0.013	-	0.08	0.001	0.38
S960QC	0.09	0.21	1.05	0.03	0.002	0.003	0.032	0.008	0.025	0.82	0.04	0.04	-	0.01	0.004	0.49
Filler material	0.08	0.60	1.40	-	-	-	0.05	-	≤0.30	0.30	2.50	0.45	-	-	-	0.45

Mechanical properties				
Materials	Yield strength (MPa)	Tensile strength (MPa)	Elongation A5 (%)	Hardness (HV5)
TMCP E500	515	620	11	240
S960QC	960	1000	18	320
Filler material	780	830	≥17	270

Table 2. Welding parameters.

Specimen	**pass 1**				**pass 2**				**Cooling time, $t_{8/5}$, (s)**
	Current (A)	Voltage (V)	Welding speed (cm/min)	Heat input (kJ/mm)	Current (A)	Voltage (V)	Welding speed (cm/min)	Heat input (kJ/mm)	
1 (S1)					203	26.6	37,5	0.8	14
2 (S2)	215	25.3	37.3	0.7	208	26.7	24	1.2	32
3 (S3)					211	26.7	18	1.8	49

Results and discussions

Fine-grain HAZ Microstructures

Figure 5 depicts an EDS scan of a welded sample on the TMCP E500 side. It is important to note that the welded sample analyzed had a heat input of 1.8 kJ/mm, which was higher than the other values. The measurement was made on the fine grain heat-affected zone (HAZ), where softening was more pronounced. The EDS images show an increase in carbon (C), chromium (Cr), manganese (Mn), and nickel (Ni) content when compared to the base metal (BM) alloying element composition. As stated in the introduction, Cr, Mn, and Ni all played important roles in determining strength in the HAZ. Increased allowing elements will have an effect on the mechanical properties of the welded joints. It should be noted from this analysis that C contains must be excluded from the analysis due to uncertainty due to the light element's character. It is important to note that the samples were polished and cleaned in an ultrasonic bath of hot C3H60 and C2H60 to remove any impurities. Another reason could be the measurement method used. In this study, the measurement method was taken point by point, with the reason being the carbon concentration at that point. [22-24] confirmed the same findings in their research. Regarding the appearance of ferrite morphology structure in the FGHAZ, as seen in Fig. 5, it can be assumed that the post-welding processes in these FGHAZ regions primarily preserve the composition of the TMCP E500 steel microstructural constituents. The rest

of the microstructure was mostly Bainite morphology, with some austenite remaining due to the increased heat input of the analyzed sample (1.8 kJ/mm).

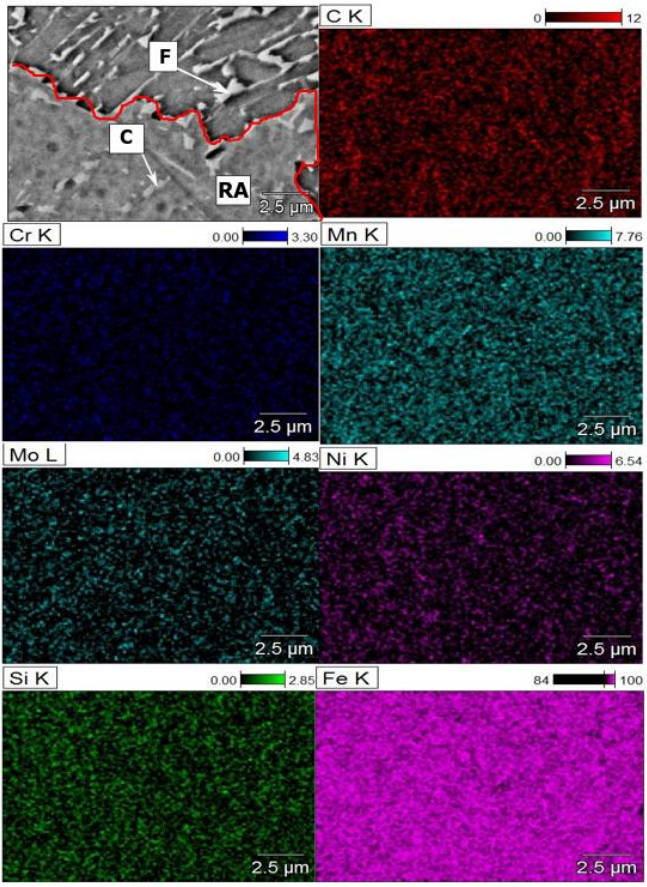

Fig. 5. EDS mapping of TMCP E500 microstructure showing CGHAZ of the steel, the weight of Carbone (C), Chromium (Cr), Manganese (Mn), Molybdenum (Mo), Nickel (Ni), Silicon (Si), and Iron (Fe).

The EDS mapping of the major alloying elements (Fe, Cr, Mn, Ni, Mo, Si) across the FGHAZ of the S960QC side of the welded sample is shown in Fig. 6. It should be noted that C is also excluded due to the uncertainty in the analysis caused by his higher character, as previously stated. It is critical to identify the phase transformation across the FGHAZ from the figure. It is visible in the microstructure as tempered martensite (TM), retained austenite (RA), and a trace of carbide (C). The presence of 2.3Cr, 0.4Si, and 2.8Mn on the FGHAZ microstructure confirms the temperature increase in that zone. This finding supports the correlation between microstructural analysis and softening in the HAZ, which can lead to the formation of a brittle zone in the welded joint. The appearance of TM, carbide (C), and some RA can explain the rise in temperature in that zone.

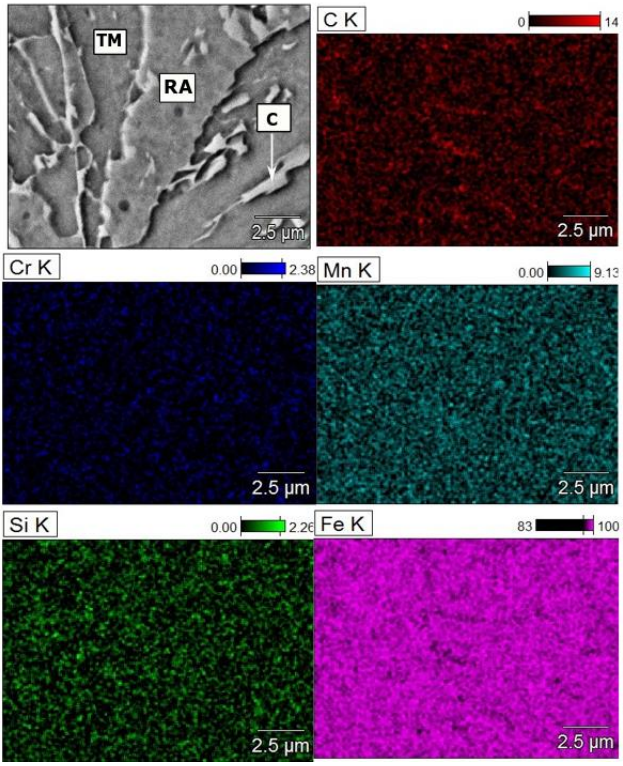

Fig. 6. EDS mapping of S960QC microstructure showing CGHAZ of the steel, the weight of Carbone (C), Chrome (Cr), Manganese (Mn), Molybdenum (Mo), Nickel (Ni), Silicon (Si), and Iron (Fe).

Mechanical properties

Microhardness profile

Figure 7 depicts the Vickers hardness distribution of dissimilar welded joints of TMCP E500/S960QC steel. When a heat input of 0.8 kJ/mm was applied (Fig. 7a), the results showed the lowest average hardness value on the TMCP E500 side. The FGHAZ had the lowest value (210 HV5) when compared to the ten recommended values of the base material, which is 280 HV5. The same results were obtained by applying a heat input of 1.2 kJ/mm (Fig. 6b). There was a slight increase in hardness on the TMCP E500 FGHAZ side. On the S960QC side, they were a little more stable. Furthermore, a decrease in hardness value can be seen, most notably in the CGHAZ of S960QC, which has developed a value of 290 HV5 compared to the base material's recommended value (320 HV5) (Fig. 7c). *Njock Bayock et al.* [25,26] and *Tasalloti et al.* [27] discovered similar results when they investigated the effect of heat input on the hardenability of dissimilar high strength and ultra-high strength steel welded joints. The FGHAZ housed the majority of their softening zone.

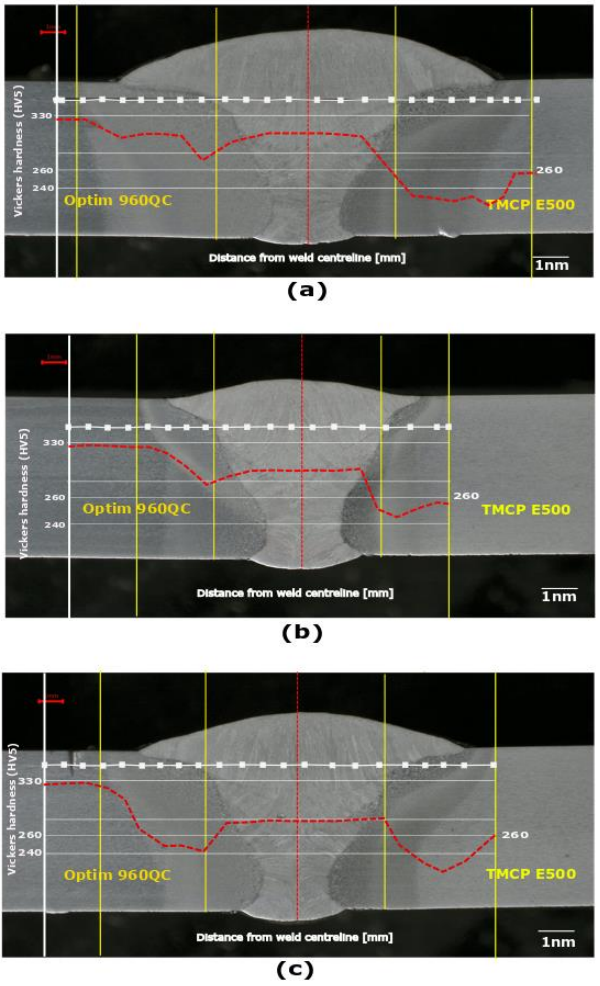

Fig. 7. Hardness profile crosses the welds samples at different heat inputs: (a) 0.8 kJ/mm, (b) 1.2 kJ/mm, and (c) 1.8 kJ/mm.

Bending test results

Figure 8 depicts the bending test results, which analyze the behavior of the welded samples. The mechanical behavior of dissimilar TMCP E500/S960QC was investigated using soft surfaces. The fracture zone was discovered in various samples. Sample 3, with a heat input of 1.8 kJ/mm (S3), produced healthy sheep. When the maximum force used was 4000N, the fracture angle was close to 149°. The fracture zone was only oriented on the fine grain heat-affected zone of the TMCP E500 area. Figure 9 depicts the bending force curve when three different welded samples were used for heat inputs of 0.8 kJ/mm, 1.2 kJ/mm, and 1.8 kJ/mm. The curvature of the different samples is quite similar in both directions at the start of the bending. The ability of different samples to distribute deformation smoothly across the bend increases with increasing angle (Fracture zone). It is important to note that the bendability of the dissimilar welded joint in terms of surface

cracking is significantly better for the bend axis in the transverse direction when a heat input of 1.2 kJ/mm is applied. When different heat inputs were used, there were not many differences in the longitudinal direction. Similar behavior was determined in the hot-rolled ultra-high-strength steel by *Kesti et al.* [28], *Deole et al.* [29], *Anna-Maija et al.* [30], and *Kaijalainen et al.* [31].

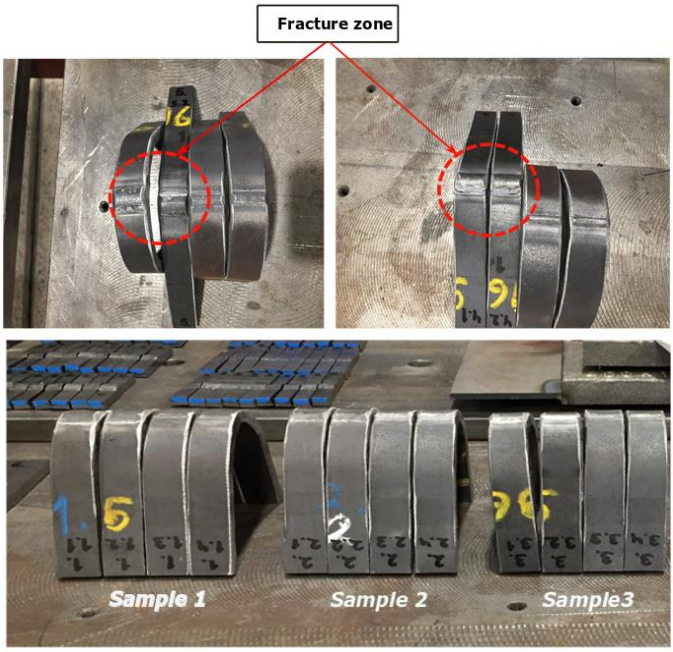

Fig. 8: Bending test results within three samples group.

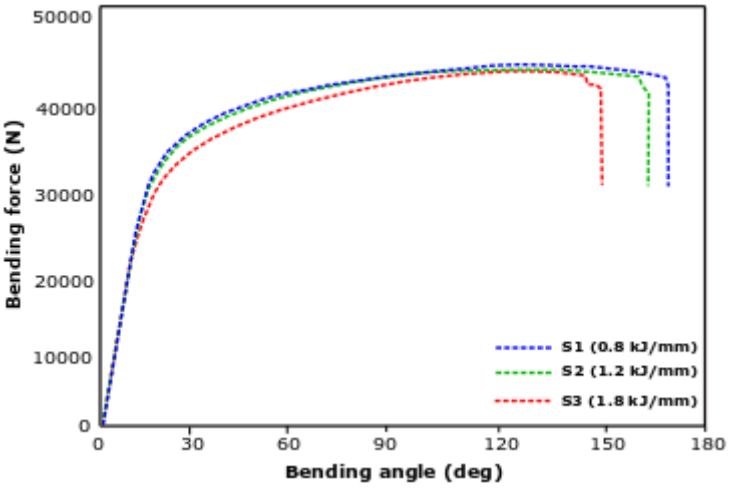

Fig. 9. Bending force of the investigated dissimilar high-strength steels.

Tensile test analysis

The tensile test was carried out in accordance with the EN ISO 6892-1: 2010 standard. Samples were collected from various heat inputs (0.8 kJ/mm, 1.2 kJ/mm, and 1.8 kJ/mm) (Fig. 10). The ZWICK / ROZ Z 330 RED test machine was used for the analysis. According to the figure, three specimens were carried out, with two samples tested for each specimen during the tensile test. The results clearly show the fracture zone, which was clearly located in the heat-affected zone of the TMCP E500 side. To be more specific, fine grain HAZ. It is supported by the hardness test results, which revealed softening in the FGHAZ of the TMCP E500 side.

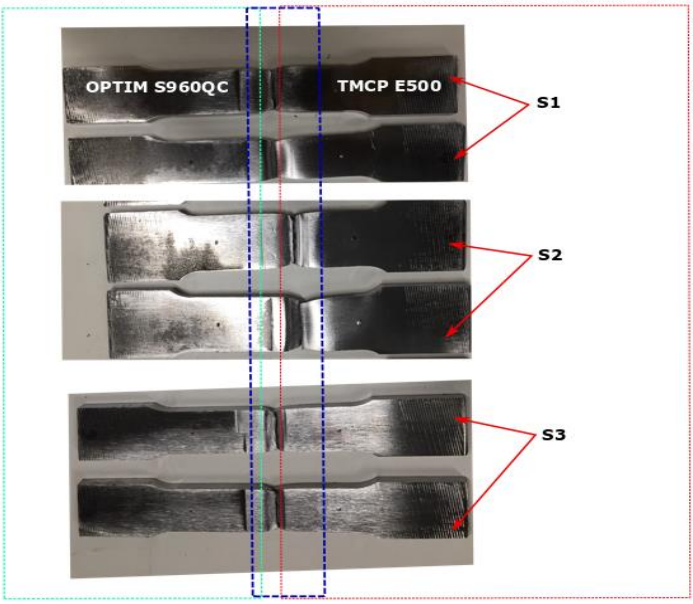

Fig. 10. The tensile test result of the fracture location in the different samples.

Table 3 shows the results of the experimental analysis. It was discovered that sample 1(S1), which had the lowest heat input (0.8 kJ/mm), developed an average yield strength (Re) of 756.1 MPa after the two tests, and an ultimate tensile strength (UTS) of 815.5 MPa. The average elongation (%) was calculated to be 9.9%. Sample 2 (S2) was the second test range, with a heat input of 1.2 kJ/mm. The results show a decrease in an average YS of 707.9 MPa and a UTS of 808.7 MPa. The average elongation (%) was calculated to be 7.8%, the lowest of S1. The final heat input used in this analysis was S3 (1.8 kJ/mm), which was significantly higher than the other values. The average yield strength was 699.5 MPa, the ultimate yield strength was 769.7 MPa, and the sudden elongation was 7.8%. It was later discovered that the requested rupture zone was the TMCP E500 HAZ. The average tensile test value for the specimen of sample S3 has been listed as low (YS 699.5 MPa, UTS 769.7 MPa), with an average elongation of 6.6%. We are presenting the most softening area in the HAZ, as demonstrated by the microhardness results. Increased heat input reduces the strength of the welded joint and can have an effect on its performance. It could be the result of the high heat input parameters, resulting

in a softening of the TMCP E500's HAZ. It is important to note that an increase in heat input of up to 1.8 kJ/mm can cause crack propagation in the HAZ. That is the way the result carry out by *Gorka et al.* [32], *Löbbe et al.* [33], *Wu et al.* [34], and *Lahtinen et al.* [35] recommended to applied post-weld heat treatment to improve the mechanical properties in the softening areas of the HAZ.

Table 3. Effect of heat input and filler metal on the mechanical behavior of the weld joint.

Sample	Dimensions (mm)	YS (MPa)	UTS (MPa)	Lo (mm)	Lu (mm)	A%	Place of rupture
S1A	25x8	759.1	817.8	79.4	87.4	10	HAZ TMCP E500
S1B	25x8	753.0	813.3	79.6	87.4	9.8	HAZ TMCP E500
Average		756.1	815.5			9.9	
S2A	25x8	715.7	794.4	79.6	85.3	7.2	HAZ TMCP E500
S2B	25x8	700	823	79.7	85	8.3	HAZ TMCP E500
Average		707.9	808.7			7.8	
S3A	25x8	692.8	769.1	79	83.8	6.1	HAZ TMCP E500
S3B	25x8	706.3	770.3	79.2	84.9	7.2	HAZ TMCP E500
Average		699,5	769.7			6.6	

Conclusion

For joining HSS and UHSS in the construction of extreme conditions for offshore structures, advanced and efficient welding technologies are unquestionably required. Research is currently being conducted to further develop these technologies as well as to discover new welding technologies that will ensure that the desired weld quality and the correlation between microstructural composition and mechanical properties are met while increasing productivity rates. The case study describes the effects of different heat inputs (0.8 kJ/mm, 1.2, 1.8 kJ/mm) on the microstructural constituents, hardenability, bendability, and strength of welded samples of TMCP E500/S960QC steel. The following observations are particularly noteworthy:

- The noticeable presence of 2.3Cr, 0.4Si, and 2.8Mn on the FGHAZ microstructure of the S960QC side confirms the increase of temperature in that zone. This finding confirms the correlation between the microstructural analyses with the softening in the HAZ which can develop a brittle zone in the welded joint. The increase of the temperature up to 1.8 kJ/mm developed the appearance of TM, carbide, and some RA during the phase transformation.

- The most softening areas were observed on the TMCP E500 side, which an average macro hardness value of 160 HV5. It is very important to pay attention to applied heat input to weld dissimilar TMCP E500-S960QC.
- Bending test results reveals the fracture angle was close to 149° when the maximum force applied was 4000N, that fracture zone was oriented exclusively in the FGHAZ which had the higher softening zone. The bendability, when observed the surface cracking on the dissimilar welded joints, was significantly better for the bend axis in the transverse direction by applying heat input of 1.2 kJ/mm during the welding process.
- Due to the sensibility of welding dissimilar HSS/UHSS materials, because of the influence of increasing heat input, it is recommended to use a heat input of 1.2 kJ/mm. Those values lead to reasonable strength and a better phase transformation in the HAZ.

It can be concluded that the weld joint quality depends on many factors such as; joint geometry, welding parameters, based materials properties, etc. the challenge is to apply the welding process in dissimilar materials and to use extreme climate conditions. These welded joints can be applied to extreme climate conditions.

Acknowledgments

The authors would like to thank the technical support from the Cameroon Welding Association (CWA).

References

[1] D. A. Porter: IIW International Conference High-Strength Materials - Challenges and Applications, Helsinki, Finland 2-3 July 2015.
[2] F. Njock Bayock, P. Kah, B. Mvola, and P. Layus: Rev Adv Mat Sci, 58 (2019) 38-49.
[3] H. Chen, J. Zhang, J. Yang, F. Ye: Int J of Cor (2018) 7169681.
[4] C. Fan, H. Wang, D. Ma: Adv in Mat Sci and Eng, 9 (2021), 9953319.
[5] W. Phanitwong, A. Sontamino, S. Thipprakmas: Adv in Mat Sci and Eng (2016) 1634840.
[6] Jr. Morris: Mat Res Society Symp, Proc, 539 (1999) 23-27.
[7] I. Gorynin, E. Khlusova: Herald of the Russian Academy of Sciences, 80 (2011) 507-513.
[8] O. Akselsen, E. Østby, C. Thaulow: Proc of ISOPE, USA, 2011.
[9] C. Lee, H. Shin, K. Park: J of Const Steel Res 74 (2012) 134-139.
[10] J-B. Yan, J. Liew, M-H. Zhang, J-Y. Wang: Mat and Des, 61 (2014) 150-159.
[11] Y. Shin, S. Kang, H. Lee: Mat Sci Eng A, 434 (2006) 1-12.
[12] C. Luru: Survey of structural steel used in major construction projects," Niobium Bearing Structural Steels, Ed. Steven Jansto and Jitendra Patel, TMS (The Minerals, Metals and Materials Society) (2010) 165-178.
[13] J. Billingham, J. Spurrier, and P.J. Kilgallon: Review of the performance of high strength steels used offshore: Res Report 105 Cranfield University (2003) ISBN 0717622053.
[14] W. Guo, D. Crowther, J.A. Francis, A. Thompson, and Z. Liu, L. Li: Mat Des, 85 (2015) 534–548.
[15] P. Layus, P. Kah, V. Gezha: Part B: J of Eng Man, 232 (2016) 114-127.

[16] T. Schaupp, W. Ernst, H. Spindler, T. Kannengiesser: Int. J. Hydrogen En, 45 (2020) 20080–20093.
[17] J. Tomków, M. Landowski, D. Fydrych, G. Rogalski: Mar Str, 81 (2022) 103120.
[18] P. Raghawendra, S. Singh, M. Gáspár: Metals, 12 (2022) 678.
[19] ISO 6892-1: 2016. International Standard Test Methods for Tensile Testing of Metallic Materials; ISO 6892-1: 2016; ISO: Geneva, Switzerland, 2016.
[20] SFS-EN ISO 7438:2016. International Standard Test Methods for Bending Testing of Metallic Materials; SFS-EN ISO 7438:2016; ISO: Geneva, Switzerland, 2016.
[21] P. Layus; P. Kah; V. Ryabov; J. Martikainen: Inter. J. Of Mech. And Mat Ing (2016) 1-4.
[22] F. Njock Bayock, P. Kah, P. Layus, V. Karkhin: Metals (355) 2019 9.
[23] S. Talas: Mat Des, 31 (2010) 2649–2653.
[24] S. Gao, L. Yuntao, L. Yang, W. Qiu: Mat Sci & Eng A, 720 (2018) 117-129.
[25] F. Njock Bayock, P. Kah, A. Salminen, B. Mvola, X. Yang: Rev Adv Mat. Sci, 59 (2020) 54-66.
[26] F. Njock Bayock, M. Kibong, S. Timba, N. Nji: Int J of Eng. & Tech (11) 2022, 1-9.
[27] H. Tasalloti, P. Kah, J. Martikainen: Mat Char (2017) 29-41.
[28] V. Kesti, A. Kaijalainen, A.Väisänen, A. Järvenpää, A. Määttä, A.-M. Arola, K. Mäntyjärvi, R. Ruoppa: Mat Sci For, 786 (2014) 818-824.
[29] A. Deole, M. Barnett, M. Weiss: AIP Conf Proc 1960 (2018) 150003.
[30] A. Anna-Maija, A. Kaijalainen, V. Kesti, L. Troive, J. Larkiola, D. Porter: Mat Today Com, 26 (2021) 101943.
[31] A. Kaijalainen, V. Kesti, L. Troive, A. Arola, T. Liimatainen, D. Porter: Met Mat Trans A 47 (2016) 4175- 4188.
[32] J. Gorka, S. Stano: Metals, 8 (2018) 1-15.
[33] C. Löbbe, O. Hering, L. Hiegemann, A. Tekkaya: Materials (2016) 1-19.
[34] W. Wu, P. Hu, G. Shen: Math Prob in Eng (2015).
[35] T. Lahtinen, P. Vilaca, P. Peura, S. Mehtonen: Appl Sci, 9 (2019) 1031.